

NEAR-INFRARED EMISSION LINES OF V723 CASSIOPEIAE (NOVA CASSIOPEIAE 1995)

RICHARD J. RUDY,¹ CATHERINE C. VENTURINI,¹ DAVID K. LYNCH,¹ S. MAZUK,¹ AND R. C. PUETTER^{2,3}

Received 2002 January 8; accepted 2002 March 31

ABSTRACT

Near-infrared spectroscopy (0.8–2.5 μm) from two epochs is presented for the very slow nova V723 Cassiopeiae (=Nova Cassiopeiae 1995). Its bright, comparatively narrow emission lines (FWHM $\sim 500 \text{ km s}^{-1}$) make it ideal for determining wavelengths of unidentified emission lines that appear in the nebular/coronal stages of novae. We present wavelengths for 16 previously unobserved or unidentified features and search for identifications by looking for coincidences with known atomic transitions. For a candidate transition, the likely abundance of the parent ion is considered and then a collisional, fluorescent, or recombination process capable of exciting the feature is sought. Four of the lines are identified in this manner, all of them collisionally excited, forbidden transitions. One of these, [Ti VII] $\lambda 22050$, is a new coronal line that de-excites directly to the ground state. Three other lines are associated with transitions from collisionally excited, low-lying, metastable levels of Fe^{+5} . Of the remaining unidentified features, five, with wavelengths of 8926, 11110, 11900, 15545, and 20996 Å, have been observed in other novae. Comparing the time development of these features with the [S VIII] $\lambda 9913$ coronal line indicates that all have parent ions of lower excitation ($< 280 \text{ eV}$) than S^{+7} .

Subject headings: infrared: stars — line: identification — novae, cataclysmic variables — stars: individual (V723 Cassiopeiae)

1. INTRODUCTION

Novae provide an astrophysical laboratory in which to observe the formation and development of exotic emission lines. Factors such as abundances rich in heavy elements, very high optical depths shortly after outburst, and excitation and ionization by a very hot source at later epochs result in emission lines that are rarely produced in other sources.

At the very earliest epochs novae will frequently display emission lines of hydrogen and other low-excitation species such as Fe II, many with P Cygni profiles. At maximum light the spectra resemble those of F stars, displaying an absorption spectrum. At slightly later times when emission lines begin to reappear, there are low-excitation features from many species in addition to H and Fe. The near-infrared spectrum displays numerous lines of N I and C I and is dominated by fluorescently excited lines of O I (see, e.g., Rossano et al. 1994; Lynch et al. 1995). As He I lines appear, P Cygni profiles on He I $\lambda\lambda 10830$ and 20581 indicate the significant optical depths in these features.

At later epochs, the ejecta in which the emission lines arise begin to disperse, and the fluorescently excited lines disappear, as do the recombination lines of neutral carbon and nitrogen. As the excitation increases, He I $\lambda 10830$ becomes the dominant line in the infrared. He II lines then appear and strengthen.

At this point the first “coronal” lines, most notably [Si VI] $\lambda 19641$ and [Ca VIII] $\lambda 23205$, begin to emerge. Some of these features were first detected in the solar corona, hence the name. Greenhouse et al. (1990) provide a working definition of coronal lines as fine-structure transitions to the ground term for species whose ionization energies exceed 100 eV. Coronal lines are the most dramatic and unusual emission lines in the high-excitation spectra of novae. The first infrared coronal lines in novae were detected by Grasdalen & Joyce (1976) and have been the topic of numerous subsequent studies (e.g., Ferland, Lambert, & Woodman 1986; Greenhouse et al. 1990, 1993; Woodward et al. 1995; Mason et al. 1996). The most recent compilation of new infrared coronal lines in novae is by Wagner & Depoy (1996, hereafter WD96), who observed the high-excitation phase of V1974 Cygni (Nova Cygni 1992). The study of coronal and other high-ionization emission lines in novae provides knowledge about the conditions within the line-forming regions as well as abundance information about the compact star, its companion, and the explosion process itself.

In this paper we present observations of V723 Cassiopeiae (Nova Cas 1995) from 1999 August and 2000 July. This nova developed very slowly (Iijima, Rosino, & Della Valle 1998) and sustained a high excitation for a sufficiently long duration that we could observe it 4 and 5 yr after outburst. In addition, it had comparatively narrow lines (FWHM $\sim 500 \text{ km s}^{-1}$) that facilitated the detection of weak features, the separation of blended features, the identification of new features, and the accurate determination of wavelengths for features that could not be identified. We measure wavelengths for 16 new or previously unidentified features and present the methodology we followed to search for their identifications. The seven lines that were associated with known transitions are discussed as well as potential transitions for the remaining features.

¹ Space Science Applications Laboratory, The Aerospace Corporation M2/266, P.O. Box 92957, Los Angeles, CA 90009; richard.j.rudy@aero.org, david.k.lynch@aero.org, stephan.m.mazuk@aero.org, catherine.c.venturini@aero.org.

² Center for Astrophysics and Space Sciences, University of California at San Diego, La Jolla, CA 92093; rpuetter@ucsd.edu.

³ Pixon LLC, 9295 Farnham Street, San Diego, CA 92123; rick.puetter@pixon.com.

2. OBSERVATIONS

The infrared spectrophotometry of Nova Cas was acquired on the nights of 1999 August 29 and 2000 July 20 (UT) with the 3 m Shane reflector of the Lick Observatory. The instrument used was the Aerospace Near-Infrared Imaging Spectrograph (NIRIS), which is described in more detail by Rudy, Puetter, & Mazuk (1999). Briefly, the spectrograph uses two channels, each containing a collimator, grating, camera, and detector array, to provide nearly continuous coverage between 0.8 and 2.5 μm . A beam splitter that switches from reflection to transmission at 1.38 μm separates the channels. The detectors are two-quadrant NICMOS3 devices providing 256 channels in the spectral dimension and 128 in the spatial. The spatial resolution is 1'' pixel⁻¹. A 600 line mm⁻¹ grating blazed at 1.0 μm operates in the “blue” channel, while a 300 line mm⁻¹ blazed at 2.0 μm services the “red.” Each channel has a nearly constant resolution, 16 Å for the blue channel and 37 Å for the red, when using the 3'' slit width employed for our observations of Nova Cas.

Because the focal plane arrays do not span the entire spectral ranges of their respective channels, each is translated to provide complete wavelength coverage. The spectrum from each channel is the result of six separate scans. Each individual blue scan covers 0.238 μm , and each red scan spans 0.465 μm . All scans oversample the spectral resolution by a factor of 2. The six individual scans are composed of three pairs of observations at three widely separated wavelength positions. Each pair consists of an observation at the nominal wavelength position and a second in which the detector array is translated 2.5 pixels from the first location. This procedure minimizes the effect of bad pixels and provides additional oversampling. The pair of scans is near the center of the spectral range and provides overlap (0.074 μm for the blue and 0.143 μm for the red channel) with the neighboring pairs of scans. This overlap facilitates the combining of the spectral pieces.

To remove the instrumental response and reduce the effects of atmospheric absorption, the data were reduced by dividing the raw spectra of V723 Cas by those of two nearby comparison stars. The comparison stars were HR 326 for the 1999 August data and HR 529 for the 2000 July observations. The former is a B8 V with $V = 5.79$, while HR 529 is an F5 IV with $V = 5.90$. To remove the intrinsic spectra of the comparison stars from the ratios, models from Kurucz (1991) that approximate the spectral type of the comparison were used. An absolute flux scale was set by normalizing to the K magnitudes of HR 326 and HR 529 of 6.04 and 4.90. The K magnitudes were calculated from the V magnitudes tabulated in the Bright Star Catalogue (Hoffleit & Jaschek 1982) and the nominal $V-K$ colors from Koorneef (1983) appropriate to their spectral types.

Line strengths were measured for the emission features using two methods: (1) by simultaneously fitting both a Gaussian line profile and a second-order continuum and (2) by interactively computing the “area” of a feature using the cursor to specify both the shape of the underlying continuum and the boundaries of the emission line. Errors in the *relative* line strengths include the formal errors from the fitting procedure but also take account of variations among the individual scans and factors such as transparency of the atmosphere and uncertainties in the levels of the nearby continuum. One strong line, [Si VII] $\lambda 24807$, has a very large

uncertainty because it lies at the red edge of our spectral range. Line strengths relative to Pa β and their errors are reported in Table 1 for both the 1999 and 2000 data. Uncertainties in the *absolute* flux level, as gauged from repeated observations of many of our program sources, are typically less than 20%.

A wavelength scale for the data was obtained in multiple ways. A scale was first derived from emission-line lamps of helium and argon and then checked against the OH lines from the night sky. Finally, the wavelength features thus determined were compared with known, nearby lines in the nova spectrum. Wavelengths (in air), together with their uncertainties, are presented in Table 2 for the new and unidentified features. Some of these features are blended with other emission lines. Their wavelengths were obtained using a least-squares fitting procedure that assumed Gaussian profiles of identical widths for each of the components. The uncertainty in the line center depends critically on the strength and proximity of the feature or features with which it is blended. An extreme case is the unidentified line at 23149 Å (see Table 2), where the feature manifests only as a blue wing on [Ca VIII] $\lambda 23208$ and, accordingly, has a large wavelength uncertainty.

3. RESULTS AND DISCUSSION

The organization of this section is as follows: In § 3.1, a brief description of the spectrum and its time development is presented, and the reddening is derived. Section 3.2 discusses the methods used to search for identifications for unknown features. Section 3.3 treats identifications for new features including a [Ti VII] line and numerous transitions ascribed to higher ionization states of iron. Section 3.4 discusses features for which no satisfactory identifications were found.

3.1. General Description of the Spectrum

In Figures 1 and 2, the 1999 August and 2000 July spectra of V723 Cas are presented. The known emission features are labeled. By the time of these observations the spectrum of V723 Cas was well into the coronal phase. The coronal lines [S VI] $\lambda 19641$ and [Ca VIII] $\lambda 23208$ were among the strongest features present in 1999 August, and the He II lines were well developed. All of the low-excitation permitted lines from C, N, and O that are common in the early time spectra of novae (see, e.g., Rossano et al. 1994; Lynch et al. 1995) had disappeared. Of the low-excitation features from the heavy elements, only the durable and ubiquitous [N I] $\lambda 10400$ remained. This description applies to the 2000 July data as well. There were, however, changes in the spectrum between the two epochs. Overall, the equivalent widths of the H I and He I lines decreased 10%–20% between the epochs, while those of some of the collisionally excited lines of lower excitation such as [S II] $\lambda\lambda 10287-10370$, [S III] $\lambda\lambda 9069, 9532$, and [N I] $\lambda 110400$ remained nearly constant or increased slightly.

The most dramatic change, which is shown explicitly in Figure 3, was the appearance of the [S VIII] $\lambda 9913$ coronal line. Its presence in the 2000 data reflects the increase in the excitation of the spectrum. In addition, the [S VIII] line together with [Al IX] $\lambda 20444$ delineate the upper energy range for photons in the ionizing spectrum. The former requires photons with energies in excess of 280 eV to form,

TABLE 1
OBSERVED EMISSION-LINE STRENGTHS OF V723 CAS

WAVELENGTH ^a (Å)	IDENTIFICATION	F / F(Paβ)	
		1999 August ^b	2000 July ^c
8140	?	...	0.048 ± 0.020
8237	He II 9-5	0.172 ± 0.030	0.181 ± 0.020
8341	?	0.032 ± 0.012	0.065 ± 0.015
8502	Pa16	0.020 ± 0.010	...
8545	Pa15	0.019 ± 0.010	...
8598	Pa14	0.029 ± 0.010	...
8665	Pa13	0.048 ± 0.015	0.041 ± 0.015
8750	Pa12	0.063 ± 0.015	0.049 ± 0.010
8797	?	0.023 ± 0.010	0.021 ± 0.007
8863	Pa11	0.095 ± 0.020	0.068 ± 0.010
8926	?	0.043 ± 0.012	0.056 ± 0.010
9015	Pa10	0.135 ± 0.015	0.101 ± 0.010
9069	[S III]	0.101 ± 0.015	0.122 ± 0.010
9229	Pa9+?	0.211 ± 0.020	0.188 ± 0.020
9345	He II 8-5	0.290 ± 0.025	0.321 ± 0.025
9532	[S III]	0.204 ± 0.050	0.315 ± 0.12
9545	Pa8	0.278 ± 0.050	0.210 ± 0.12
9711	C III	0.024 ± 0.009	0.024 ± 0.010
9762	He II 15-6	0.032 ± 0.009	0.030 ± 0.010
9850	[C I]?	0.024 ± 0.010	...
9913	[S VIII]	<0.010	0.273 ± 0.020
10049	Paδ	0.414 ± 0.070	0.332 ± 0.030
10124	He II 5-4	2.13 ± 0.20	2.23 ± 0.060
10287-10370	[S II]	0.073 ± 0.020	0.122 ± 0.020
10400	[N I]	0.218 ± 0.020	0.378 ± 0.020
10777	?	0.038 ± 0.020	0.063 ± 0.020
10830	He I	8.96 ± 0.30	6.32 ± 0.30
10938	Paγ	0.533 ± 0.060	0.547 ± 0.060
11104	?	0.052 ± 0.015	0.054 ± 0.015
11132	?	0.040 ± 0.015	0.046 ± 0.015
11626	He II 7-5	0.461 ± 0.020	0.458 ± 0.020
11673	He II 11-6	0.079 ± 0.015	0.073 ± 0.015
11900	?	0.045 ± 0.010	0.039 ± 0.010
11969	He I	0.012 ± 0.008	...
12332	?	0.061 ± 0.010	0.057 ± 0.010
12528	He I	0.016 ± 0.008	0.029 ± 0.015
12676	?	0.108 ± 0.015	0.094 ± 0.015
12785, 12790	He I	0.033 ± 0.015	0.073 ± 0.020
12818	Paβ	1.000	1.000
12893	?	0.042 ± 0.010	0.046 ± 0.025
13076	?	0.037 ± 0.010	<0.010
14760	He II 9-6	0.136 ± 0.015	0.113 ± 0.015
14882	He II 14-8	0.031 ± 0.012	0.025 ± 0.010
15342	Br18	0.007 ± 0.004	...
15439	Br17	0.011 ± 0.004	...
15545, 15556	? + Br16	0.039 ± 0.006	0.032 ± 0.008
15701, 15719	Br15 + He II 13-7	0.050 ± 0.006	0.036 ± 0.008
15881	Br14	0.021 ± 0.005	0.012 ± 0.004
16109	Br13	0.026 ± 0.006	0.021 ± 0.004
16407	Br12	0.042 ± 0.006	0.047 ± 0.004
16806	Br11	0.050 ± 0.006	0.051 ± 0.004
16915	He II 12-7	0.043 ± 0.006	0.044 ± 0.004
17002	He I	0.015 ± 0.006	0.029 ± 0.005
17155	[Ti VI]	0.086 ± 0.010	0.091 ± 0.010
17362, 17356	Br10 + [P VIII]?	0.080 ± 0.010	0.090 ± 0.008
18174	Br9	0.106 ± 0.025	0.099 ± 0.025
19446	Br8	0.129 ± 0.020	0.117 ± 0.020
19641	[Si VI]	5.74 ± 0.50	5.74 ± 0.50
20373	He II 15-8	0.033 ± 0.005	0.033 ± 0.006
20444	[Al IX]	0.012 ± 0.005	0.029 ± 0.006
20581	He I	0.066 ± 0.010	0.060 ± 0.010
20996	?	0.014 ± 0.005	0.020 ± 0.005
21120, 21132	He I	0.010 ± 0.005	0.014 ± 0.005
21655	Brγ	0.184 ± 0.015	0.186 ± 0.012

TABLE 1—Continued

WAVELENGTH ^a (Å)	IDENTIFICATION	F / F(Paβ)	
		1999 August ^b	2000 July ^c
21882	He II 10-7	0.073 ± 0.015	0.076 ± 0.015
22050	?	0.041 ± 0.008	0.069 ± 0.010
22188	?	0.013 ± 0.008	0.023 ± 0.007
23149	?	0.150 ± 0.060	0.318 ± 0.060
23205	[Ca VIII]	1.33 ± 0.080	3.19 ± 0.15
23464	He II 13-8	0.028 ± 0.007	0.028 ± 0.020
24807	[Si VII]	1.39 ± 0.40	2.40 ± 0.50

^a Laboratory wavelengths as measured in air.
^b $F(\text{Pa}\beta) = 6.22 \times 10^{-13} \text{ ergs cm}^{-2} \text{ s}^{-1}$.
^c $F(\text{Pa}\beta) = 3.60 \times 10^{-13} \text{ ergs cm}^{-2} \text{ s}^{-1}$.

while the value for the latter is 285 eV. The comparative weakness of the [Al IX] feature suggests that photon energies do not greatly exceed its ionization threshold, while a firm upper limit is set by the absence of [S IX] λ12520 (energy >328 eV), [Fe XII] λλ10747, 10798 (>331 eV), and [Si X] λ14301 (>351 eV).

At both epochs, the Br10 feature (17362 Å) was overly strong relative to the other Brackett lines, indicating that it was blended with an additional feature. WD96 suggested that [P VIII] λ17356 served this role in V1974 Cygni (Nova Cyg 1992). With a photon energy greater than 263 eV necessary to produce this species, it lies near but does not exceed the upper range of energies confirmed in V723 Cas. Unfortunately, our spectrum does not include the [P VII] λ13746 feature that would confirm the presence of emission from high-ionization states of phosphorous. An additional possibility is [Sc IX] λ17353, a line that requires photon energies of only 159 eV to form its parent ion. It is a true ground-state transition and should be detectable if the elemental abundance of scandium is sufficiently large. Unfortunately, there are no additional [Sc IX] lines and a near absence of other scandium features in the near-infrared that might confirm its presence.

TABLE 2
NEW AND UNIDENTIFIED LINES

Measured Wavelength ^a (Å)	Identification
8140 ± 4	[Fe V] λ8137
8341 ± 2	[Fe V] λ8343
8797 ± 2	[Fe V] λ8800
8926 ± 2	?
10777 ± 6	[Fe IV] λ10761, 10775?
11104 ± 6	?
11132 ± 6	[Fe IV] λ11133?
11900 ± 4	?
12332 ± 2	[Fe VI] λ12330
12676 ± 4	[Fe VI] λ12674
12893 ± 6	[Fe VI] λ12888
15545 ± 10	?
20996 ± 6	?
22056 ± 7	[Ti VII] λ22050
22188 ± 8	[Fe III] λ22178?
23149 ± 15	?

^a Wavelength in air.

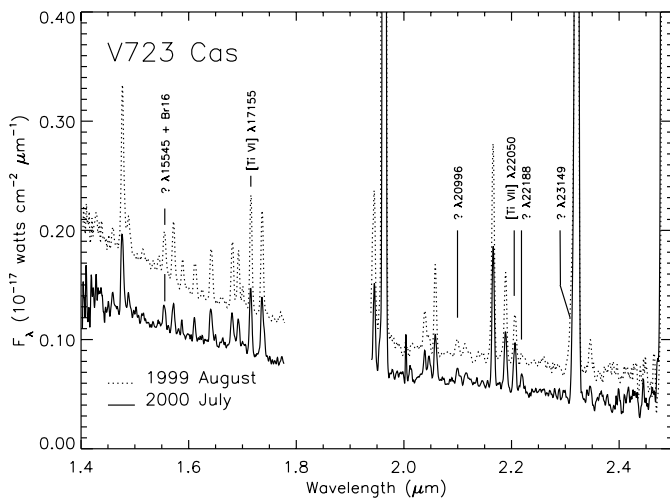


FIG. 5.—1999 August and 2000 July spectra of V723 Cas from 1.4 to 2.5 μm showing the new and unidentified lines. The [Ti vi] $\lambda 17155$ line, discovered previously in V1974 Cygni (Nova Cygni 1992), is shown for comparison with the newly detected [Ti vii] $\lambda 22050$ feature. Lines with question marks either remain unidentified or have an identification that is uncertain. The features at 15545 and 20996 \AA have been in other novae.

labeled are presented in Figures 4 and 5. Those lines for which identifications are presented are considered in the next section; the unidentified lines are discussed in § 3.4.

Once a wavelength was determined for a feature, an identification was searched for by looking for coincidences with transitions in the on-line tables of R. Kurucz, the University of Kentucky, and the National Institute of Standards (NIST). All these sources are based on the extensive tables of energy levels compiled by NIST. All present electron configurations, types of transition (electric dipole or quadrupole, magnetic dipole), upper and lower energy levels and their associated angular momentum, and in many cases, transition probabilities. From the numerous matches within twice the error range given for the measured wavelength in Table 2, we looked for ions of astrophysically prevalent elements at low, moderate, and high levels of ionization. Among these, we first sought transitions between low-lying levels that could be readily excited by collisions but then also considered levels up to $\sim 60,000 \text{ cm}^{-1}$ above the ground state. Transitions of this type were overwhelmingly forbidden transitions (i.e., not electric dipole transitions). Of these, we looked for transitions with sufficiently high A -values that collisional de-excitation was minimal for a 10^5 cm^{-3} gas. This assumption excluded electric quadrupole transitions but resulted in numerous candidate magnetic dipole transitions. Several emission lines of this type from various ionization states of iron were found to match features in the spectrum of V723 Cas (see below). For these, we constructed multilevel atoms to check whether the relative strengths of the candidate features were consistent with the observations.

We also considered collisionally excited transitions from elements with $Z > 30$ (i.e., from elements higher than zinc) that are less abundant. The merit of this approach has been demonstrated by Dinerstein (2001), who found, in planetary nebulae, coincidences between two unidentified infrared lines and ground-state transitions of Kr III and Se IV. We computed transitions among energy levels within $60,000 \text{ cm}^{-1}$ of the ground state for the ions for which NIST had

compiled energy levels but found no likely matches to the lines of Table 2.

For the features that did not have candidate transitions that could be collisionally excited, we then looked for fluorescent paths among high-level permitted transitions. For the exciting lines causing the fluorescence, we considered resonant lines of H I, He I, and He II. The only possible identification that resulted from transitions of this type was Ne II $\lambda 8797$, which is excited from the ground state by He II $\lambda 303.78$ in a process identical to the Bowen fluorescence that produces the ultraviolet O III lines (Osterbrock 1989, p. 107). This is discussed in § 3.4.2.

If neither collisionally nor fluorescently excited lines could be matched to an unidentified emission feature, we then examined permitted lines to see if recombination processes could result in features of the necessary strength to match the observations. When matches were found, we searched for companion lines that were expected to be comparable or greater in intensity. We also considered transitions among very high n -levels of common ions where the energies of states with different angular momenta are very similar. Such transitions are common in the infrared Wolf-Rayet stars, originating from high ionization states of C, N, and O (Eenens, Williams, & Wade 1991; Figer, McLean, & Najarro 1997).

3.3. New Lines and Iron Lines

The new lines with secure identifications are discussed in this section. These include [Ti vii] $\lambda 22050$ together with multiple transitions of [Fe vi]. Candidate transitions from [Fe v], [Fe iv], and [Fe iii] are also discussed in this section. Features that remain unidentified are treated in § 3.4.

3.3.1. [Ti vii] $\lambda 22050$

The [Ti vii] $\lambda 22050$ feature is the only new coronal line to be identified in V723 Cas. It is a true ground-state transition that is collisionally excited. A partial Grotrian diagram illustrating the transition is presented in Figure 6. This presence of the [Ti vi] $\lambda 17155$ line in the spectrum helped to confirm this identification, and its Grotrian diagram is also included in Figure 6. The [Ti vi] feature was first identified in V1974 Cygni by WD96 and helped establish the presence of detectable titanium in novae.

The other transitions of [Ti vii] that are labeled in the Grotrian diagram of Figure 6 have radiative lifetimes similar to $\lambda 22050$ and could be observable for certain temperatures and densities. Unfortunately, collision strengths have not been computed, so we cannot perform a rigorous calculation of the relative line strengths. However, Galavis, Mendoza, & Zeppen (1995) have computed collision strengths for A III, K IV, and Ca V, ions that fall along the same isoelectronic sequence. To obtain a *qualitative* estimate of the line ratios, we use their values for K IV together with the energy levels and A -values for [Ti vii] tabulated by NIST to compute a five-level atomic model. In particular, we find that the ratio of $\lambda 4143$ to $\lambda 22050$, for electron temperatures around 10^4 K , should provide a useful diagnostic of density, varying from about a tenth to unity for densities ranging from 10^6 to 10^8 cm^{-3} .

The entries in Table 1 hint at a slight increase in the [Ti vi] line and a larger increase in [Ti vii], presumably reflecting the hardening of the ionizing spectrum. However, at neither epoch did we see the [Ti ix] $\lambda 24013$ line. This is formed by a

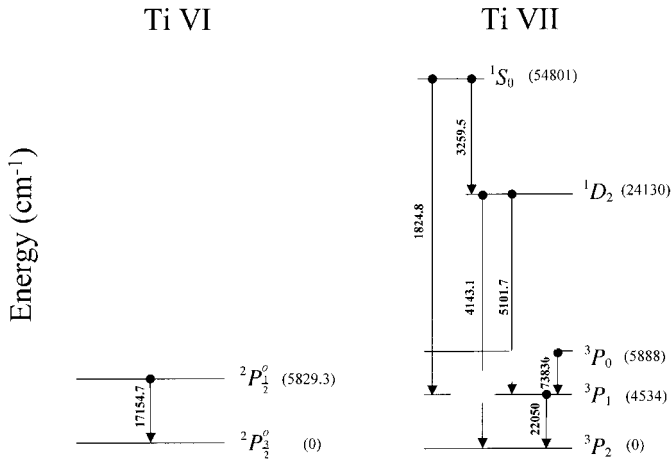


FIG. 6.—Partial Grotrian diagrams for Ti VI and Ti VII showing the strongest transitions. V723 Cas is the first object for which the [Ti VII] $\lambda 22050$ coronal line has been reported; [Ti VI] $\lambda 17155$ was discovered in the spectrum of V1974 Cygni (Nova Cygni 1992) by WD96. For Ti VII, there is another transition, between the $J = 0$ and $J = 2$ levels of the ground term that falls in the near-infrared (16979 \AA). However, it is an electric quadrupole transition that has an Einstein A -value that is 4 orders of magnitude smaller than $\lambda 22050$ and so is not seen. The other transitions shown have transition probabilities similar to $\lambda 22050$ and should be detectable. In particular the ratio of the optical line $\lambda 4143$ to $\lambda 22050$ could provide a useful gauge of densities in the 10^6 – 10^8 cm^{-3} range. With regard to [Ti VI], the transition shown is the only transition within the ground term and the only transition at all that produces an optical or an infrared photon—the next level is more than $196,000 \text{ cm}^{-1}$ above the ground state.

transition within the ground term and probably should have been detectable if significant amounts of Ti^{+8} were present. Since this requires photon energies of only 193 eV, well below the range necessary to produce the [S VIII] feature, this may indicate that titanium was not present in significant amounts in those portions of the ejecta reaching the highest levels of ionization.

3.3.2. [Fe VI] $\lambda\lambda 12330, 12674, \text{ and } 12888$

The combination of three distinct features with well-measured wavelengths makes the association of $\lambda\lambda 12330, 12674, \text{ and } 12888$ with [Fe VI] transitions the most secure of any of the identifications with the iron ions. In addition, the strengths of the features relative to the H I and He II lines did not change noticeably between the two epochs, indicating only a moderate state of excitation for the parent ion, commensurate with the 79 eV photon energies necessary to produce Fe^{+5} . None of these [Fe VI] features arise from direct transitions to the ground term, but all descend from upper levels with energies less than $30,000 \text{ cm}^{-1}$ above the ground state that can be populated collisionally at typical nebular temperatures. The only complication in associating these transitions with those of [Fe VI] is that there are numerous other infrared transitions from levels of similar energies whose strengths relative to the detected features need to be compared with the measured spectrum. Fortunately, recent calculations of the atomic parameters for Fe^{+5} allow us to compare the observed, relative line strengths with calculated values. Using the A -values from Chen & Pradhan (2000) and the collision strengths from Chen & Pradhan (1999), we have computed the populations for the lowest 19 levels (up to $72,000 \text{ cm}^{-1}$ above the ground state) and the resulting spectrum. We were unable to produce a close match to the three observed [Fe VI] lines.

Whether this is due to blending with other features, problems with the calculations, or an error with the actual line identifications is unclear. As a rough check on the model calculations, we computed line ratios for $T_e \sim 20,000 \text{ K}$ and $N_e \sim 5 \times 10^6 \text{ cm}^{-3}$, the electron temperature and density combination, respectively, that produced the best match to the three near-infrared lines. Values for the stronger optical and infrared transitions, calculated at this temperature and density, are presented in Table 3. All of the optical lines listed are seen in the spectrum of the RR Tel (Crawford et al. 1999), a symbiotic nova with a very rich emission-line spectrum. However, the prominence of the optical lines is the one aspect that raises some doubt about the identification of the three infrared features with Fe^{+5} . We are unaware of any detection of the optical [Fe VI] lines listed in Table 3 in novae. This is surprising since they should be strong for a range of temperatures and densities. However, coordinated optical and infrared observations should confirm or deny the identifications with Fe^{+5} .

3.3.3. [Fe V], [Fe IV], and [Fe III]

Like Fe^{+5} , the ions $\text{Fe}^{+4}, \text{Fe}^{+3}, \text{ and } \text{Fe}^{+2}$ all have several low-lying metastable levels that can be collisionally excited. These levels are connected by a multitude of forbidden transitions, many of which fall within the wavelength range of our observations, and most of which are not detected. However, because several of the unidentified features of Table 2 have wavelength coincidences with transitions of these ions and because of the likely presence of [Fe VI] lines and the tentative identification of [Fe III] $\lambda 22178$ in V1974 Cygni by WD96, we consider each of these ions in turn. (Fe^+ is not treated because of the absence of the strong forbidden lines at 12567 and 16435 \AA .) As with Fe^{+5} in the previous section, we compute multilevel models for these ions in order to check whether the observed features are expected to be the strongest features of the parent ion.

We computed the relative line strengths for transitions from the lowest 32 levels of the Fe^{+4} ions using the transition probabilities of Nahar et al. (2000) and collision strengths kindly provided in advance of publication by K. Berrington. A summary of the calculated strengths for the lines matching the observed infrared features and the strongest optical transitions are presented in Table 4. The calculations neither confirm nor rule out the associations of

TABLE 3
PREDICTED LINE STRENGTHS FOR SELECTED
INFRARED AND OPTICAL [Fe VI] TRANSITIONS

Wavelength ^a (\AA)	$I / I(\lambda 5176)^b$
3662	0.41
4967	0.43
4972	0.39
5146	0.40
5176	1.00
12330	0.048
12674	0.057
12888	0.023
13493	0.075

^a Wavelength in air.

^b Line ratios for $T_e = 20,000 \text{ K}, N_e = 5 \times 10^6 \text{ cm}^{-3}$.

TABLE 4
PREDICTED LINE STRENGTHS FOR SELECTED
INFRARED AND OPTICAL [Fe v] TRANSITIONS

Wavelength ^a (Å)	$I / I(\lambda 4658)^b$
3839	0.49
3891	1.00
3895	0.50
4071	0.50
4181	0.23
8137	0.051
8343	0.062
8800	0.063
10400	0.066

^a Wavelength in air.

^b Line ratios for $T_e = 12,000$ K, $N_e = 1 \times 10^6$ cm⁻³.

the three observed infrared features with [Fe v] transitions. However, the weakness or absence of [Fe v] features at 20396 and 20467 Å in the observed spectrum does require high electron densities ($\sim 10^8$ cm⁻³) and temperatures ($\sim 20,000$ K) if the association with [Fe v] is correct.

For Fe⁺³, the transition probabilities of M. A. Bautista (2001, private communication) and Bautista & Kallman (2001) and the collision rates of Zhang & Pradhan (1997) were employed in the multilevel model for this ion. Again, the NIST values were used for the 33 energy levels, extending up to 82,897 cm⁻¹, that were incorporated into the model. The stronger optical and infrared lines for this ion are listed in Table 5. The existence of [Fe iv] in the spectrum is not obvious. The calculations indicate that the combination of $\lambda 10761$ and $\lambda 10773$ comprises the strongest feature in the near-infrared, and it may well be the bump seen on the blue wing of He I $\lambda 10830$. The line at 11133 Å coincides with one of the lines of Table 2, but the features at 11579 and 12017 Å, which are predicted to have comparable strength, are not seen. Therefore, the existence of [Fe iv] features in the spectrum of V723 Cas is not clearly established.

To compute the multilevel model for Fe⁺², we used the transition probabilities of Nahar & Pradhan (1996) and the collision rates of Zhang (1996). Thirty-four levels whose val-

TABLE 5
PREDICTED LINE STRENGTHS FOR SELECTED
INFRARED AND OPTICAL [Fe iv] TRANSITIONS

Wavelength ^a (Å)	$I / I(\lambda 4907)^b$
4152	0.52
4198	0.77
4903	0.46
4907	1.00
5234	0.63
9394	0.044
10761	0.059
10775	0.031
11133	0.031
11579	0.041
12017	0.032

^a Wavelength in air.

^b Line ratios for $T_e = 12,000$ K, $N_e = 1 \times 10^6$ cm⁻³.

TABLE 6
PREDICTED LINE STRENGTHS FOR SELECTED
INFRARED AND OPTICAL [Fe iii] TRANSITIONS

Wavelength ^a (Å)	$I / I(\lambda 4658)^b$
4658	1.00
4702	0.50
4734	0.23
5270	0.62
9701	0.082
9942	0.053
22178	0.054
22421	0.053
23479	0.036

^a Wavelength in air.

^b Line ratios for $T_e = 12,000$ K, $N_e = 1 \times 10^6$ cm⁻³.

ues were taken from the NIST compilation and that range up to 57,222 cm⁻¹ above the ground state were included. Table 6 presents a selection of the strongest infrared and optical lines. Based on those values, there are no features in the spectrum of V723 Cas that can be associated unequivocally with [Fe iii]. The only likely candidate is [Fe iii] $\lambda 22178$, which might be the unidentified feature at 22188 Å. Therefore, we defer the discussion of [Fe iii] until the section dealing with that feature.

In summary, while there are several wavelength coincidences of emission lines in the infrared spectrum of V723 Cas with transitions of [Fe v], [Fe iv], and [Fe iii], the actual identifications with these transitions are uncertain. However, all of these iron ions have strong optical lines whose presence or absence in future novae should establish or rule out these identifications.

3.4. Unidentified Lines

Before beginning the discussion of the individual lines without identifications, it is worthwhile to consider the changes in line strengths with respect to Pa β between the two epochs (see Table 1). As noted above, [S viii] $\lambda 9913$ defines the highest excitation observed in V723 Cas (~ 280 eV). The appearance of this line between 1999 August and 2000 July (see Fig. 3) indicates that the excitation was below this level at the earlier epoch. All of the unknown features were present in the 1999 spectrum, and none increased nearly as dramatically as [S viii] $\lambda 9913$, suggesting that their parent ions are all of lower excitation than S⁺⁷.

We have observed several of these unidentified lines in other novae ($\lambda\lambda 8926, 11118, 11900, 15545, \text{ and } 20996$). Most of these data have not yet been published, with the exception being Nova Sagittarius 1998 (Lynch et al. 2001; the wavelengths reported for that broad-lined object were derived from these measurements of V723 Cas). In addition, WD96 reported features that probably correspond to the lines at 11900, 15545, and 20996 Å. The point here is that these lines may be present at some stage in the spectral development of many novae and for that reason are important.

3.4.1. $\lambda 8797$

As discussed in § 3.3.3, our nominal identification for this line is [Fe v] $\lambda 8800$. However, it is possible that there is con-

tribution from Ne II $\lambda 8795$, so we will discuss that feature here. Ne II $\lambda 8795$ is actually comprised of four individual lines, from two separate levels, that all lie within 0.4 Å of each other. These are permitted transitions that are fluorescently excited by He II $\lambda 303.78$ (vacuum wavelength). Ne II has two resonant transitions (to the $^2D_{3/2}$ and $^2D_{5/2}$ levels at 329,148.80 and 329,148.67 cm^{-1} , respectively) that fall within 0.03 Å of the line center of the He II transition. Absorption of the plentiful He II photons directly populates the two upper levels that produce the four Ne II transitions. To search for additional evidence of this fluorescent process, we checked for lines at 8150, 8160, 8704, and 8831 Å that also are transitions from these levels. Values for their oscillator strengths, from the compilation of Kurucz, indicate that the first three lines should have been detectable if the fluorescence process contributed significantly to the observed feature. The weakness of the process in V723 Cas may be due to the bulk of the neon existing in higher ionization states. In any case, there are other coincidences of Ne II transitions with unidentified features ($\lambda\lambda 11104, 20996$) that can be ruled out from the weakness of Ne II $\lambda 8795$. More generally, $\lambda 8795$ should probably be the strongest Ne II feature in the near-infrared when He II emission is present and is thus a good indicator of the presence of this ion. Although not significant in V723 Cas, given the general strength of the He II lines and the frequent enrichment of neon in novae, this fluorescent excitation may be an important process in other novae.

3.4.2. $\lambda 8926$

This is the first of the unidentified features seen in other novae. For this line, there are coincidences with transitions of N v and O v. Both have candidate transitions from extremely high energy levels (766,866 and 843,270 cm^{-1} , respectively). Both are ruled out by the absence of other features from the same upper levels and features from lower levels that are expected to be stronger. There is also a transition of Ar II ($^4P-^4D^0$, 147228.05–158428.11 cm^{-1}) at 8926 Å, but the companion feature at 9151 Å from the same upper level is absent. Although there are several other coincidences with this wavelength, we could identify no other realistic candidates for this feature.

3.4.3. $\lambda\lambda 11104, 11132$

This is the second of the features seen in other novae. In the other novae, all of which have broad lines, it appears as a single peak, but in V723 Cas it seems to be formed from two lines of similar strength. A possible identification for longer wavelength component remains [Fe IV] $\lambda 11133$, but the problems with this association have been presented in § 3.3.3.

There are also iron features in the vicinity of the shorter wavelength component, namely, the $b^4F_{7/2}-b^2F_{5/2}$ transition [Fe II] $\lambda 11106$ and $a^3F_2-a^3D_3$ [Fe III] $\lambda 11107$. We rule out the former based on the absence of any of the strong [Fe II] lines (e.g., $\lambda\lambda 12567, 16638$). The [Fe III] line is excluded from our multilevel model, which yields a strength for $\lambda 11107$ of less than 1% of [Fe III] $\lambda 22178$.

Another potential source for the line is N v. There are 11 transitions between the $n=9$ and $n=8$ levels that fall between 11087 and 11114 Å. The principal argument against this association is the nondetection of N v $\lambda\lambda 15059, 15184, \text{ and } 15234$. These transitions among $n=3$ levels are

expected, in a capture/cascade process, to be the strongest in the near-infrared. Whether these lines would be stronger individually than the sum of the 9–8 transitions is not clear. In addition, the 9–8 transitions do not account for the red component of the feature. An argument in favor of the association is the clustering of a second set of N v lines around the unknown feature at 15545 Å (see below). For this reason, N v remains a possibility for at least a portion of the feature.

3.4.4. $\lambda 11900$

WD96 suggested an identification of a similarly located feature in V1974 Cygni with an O VI transition at 11892 Å. This permitted transition arises from a small n -level in the O⁺ ion and is probably strong in WO-type Wolf-Rayet stars. However, it is only one of three transitions from a common upper term. Its companion lines are $\lambda\lambda 11744$ and 11965, which are weaker but should still be detectable. They are absent in V723 Cas.

There is also a feature of C IV that appears around this wavelength in carbon-rich Wolf-Rayet stars. This is one feature mentioned above that is formed from multiple, closely spaced angular momentum states with the same principal quantum number, in this case between the $n=10$ and $n=9$ levels. However, the absence of the many $n=9$ to $n=8$ transitions that cluster around 1.79 μm and the three strong $3p^2P^0-3d^2D$ lines at 20700, 20796, and 20836 Å, all of which are strong in early-type, carbon-rich Wolf-Rayet stars (Eeneens et al. 1991; Figer et al. 1997), excludes this association.

3.4.5. $\lambda 15545$

This is another line that is prominent in the spectra of novae during their coronal stage. WD96 observed this feature in Nova Cyg 1992 and suggested [Cr XI] $\lambda 15514$ as a possible identification. However, the disparity with the observed wavelength is too great for this to be the correct identification. Moreover, our data show no sign of the companion [Cr XI] feature at 18059 Å.

There are 10 transitions between 15532 and 15537 Å from the 10–9 levels of N v. The arguments for and against this association are the same as those made for the 9–8 transitions above, and for the same reasons, N v remains a possible source of this feature. There is a [Cu V] transition from the $^2P_{1/2}$ level at 28,366.60 cm^{-1} that falls at the correct wavelength that could easily be excited by collisions, but other near-infrared [Cu V] transitions from similarly placed levels are not seen.

3.4.6. $\lambda 20996$

WD96 suggested a possible identification for this feature as [Mn XIV] $\lambda 20894$. This transition is much too far from our measured wavelength. Moreover, it descends from an upper level more than 200,000 cm^{-1} above the ground state, so it cannot be collisionally excited in a 10,000–20,000 K medium. There is an N v line at 20985 Å that is ruled out for the absence of companion lines from the same upper level and stronger lines from lower levels (see the arguments in the section above). An Ne II line at 20986 Å is excluded for the reasons discussed in § 3.4.1. There are two C I features: at 20991 Å ($^1D^0-^1D_2$) and at 20998 Å ($^3D_2-^3F^0_3$). However, there are several stronger transitions of C I that are not seen in V723 Cas, and it is unlikely that neutral carbon could sur-

vive in significant amounts in the relatively high excitation environment present at the time of our observations.

3.4.7. $\lambda 22188$

This line was also observed in V1974 Cygni by WD96, who identified it as [Fe III] $\lambda 22178$ along with two other transitions of [Fe III] ($\lambda\lambda 21451$ and 23479). However, they noted the absence of the companion line at 22421 \AA , a feature seen in both the Orion Nebula (Osterbrock, Tran, & Villeux 1992) and the Galactic center (Lutz, Krabbe, & Genzel 1993). The ratio of these lines has been calculated by Nahar & Pradhan (1996), who find that for a wide range of densities, $\lambda 22421/\lambda 22178 \geq 0.6$. Our 34-level model (see § 3.3.3) agrees with this result. However, although we find that while $\lambda 22178$ is often the strongest line in the near-infrared, for a plausible range of temperatures and densities, it is exceeded by [Fe III] $\lambda 9701$. We do observe a feature at about this wavelength that we have tentatively attributed to C III. We do not, however, detect $\lambda 22421$ or any other possible [Fe III] features. Together with the fact that the observed line center is significantly displaced from the laboratory wavelength, we conclude that the feature is probably not due to [Fe III].

3.4.8. $\lambda 23149$

This feature is blended with the much stronger [Ca VIII] $\lambda 23205$ line and appears on the latter's blue wing at both epochs. It is possible that it is not a distinct feature but simply an asymmetry in the [Ca VIII] line. However, because such an asymmetry is not seen on any other features, we consider it as a separate line. The wavelength, which was obtained by deconvolving the feature from the [Ca VIII] line, is very uncertain.

Given the nondetection of Pfund series lines down to Pf18, the feature is much too strong to be Pf40, although it lies almost exactly at the nominal wavelength yielded by our deconvolution. Likewise, He II lines throughout the spectrum indicate that the 20–9 transition at 23136 \AA is too weak to account for the observed feature. There is also a complex of three Na I permitted lines, all from the $^2P^0$ term at $41,355$

cm^{-1} , all within 0.2 \AA of each other, and all at the nominal wavelength. However, there are additional Na I infrared features that are not seen, and it is doubtful that an atom as fragile as sodium, with an ionization potential of 5.1 eV , could remain neutral in regions surrounding V723 Cas. There is also an [Ni VI] transition at the nominal wavelength, but this is excluded by the absence in other lines of [Ni VI] and of any transition from any ionization state of nickel.

4. SUMMARY AND CONCLUSIONS

Near-infrared spectroscopy of the narrow-line nova V723 Cassiopeiae (Nova Cas 1995) from two different epochs has provided accurate wavelengths for a number of emission lines. One new coronal line, [Ti VII] $\lambda 22050$, has been identified. There are three features that are probably due to collisionally excited, forbidden transitions of Fe^{+5} and several others that may be due to the same type of transitions in Fe^{+2} , Fe^{+3} , and Fe^{+4} . All of these iron ions have stronger companion lines at visual wavelengths, so simultaneous observations at optical and infrared wavelengths should prove or disprove these identifications. Emission features that remain unidentified and have been seen in other novae appear at 8926 , 11118 , 11900 , 15545 , and 20996 \AA .

We are grateful to A. Tullis, K. Baker, and W. Earthman, the telescope operators at the Lick Observatory during these measurements, and to T. Armstrong for their help in acquiring the data. We also would like to thank M. Bautista, A. Pradhan, K. Berrington, and their collaborators on the Iron Project for providing A -values and collisional strengths for the iron ions discussed in this paper. An anonymous referee provided several useful comments. This work was supported by the Independent Research and Development program at The Aerospace Corporation. R. C. P. acknowledges support from NASA and Pixon LLC. This work made extensive use of the atomic line lists at the National Institute of Standards, the University of Kentucky (<http://www.pa.uky.edu/~peter/atomic>), and of R. L. Kurucz and B. Bell.

REFERENCES

- Bautista, M. A., & Kallman, T. R. 2001, *ApJS*, 134, 139
 Chen, G. X., & Pradhan, A. K. 1999, *A&AS*, 136, 395
 ———. 2000, *A&AS*, 147, 111
 Crawford, F. L., McKenna, F. C., Keenan, F. P., Aller, L. H., Feibelman, W. A., & Ryan, S. G. 1999, *A&AS*, 139, 135
 Dinerstein, H. L. 2001, *ApJ*, 550, L223
 Draine, B. T. 1990, in Proc. 22nd Eslab Symposium on Infrared Spectroscopy in Astronomy, ed. B. H. Kaldeich (ESA SP-290; Paris: ESA), 93
 Eenens, P. R. J., Williams, P. M., & Wade, R. 1991, *MNRAS*, 252, 300
 Ferland, G. J., Lambert, D. L., & Woodman, J. H. 1986, *ApJS*, 60, 375
 Figer, D. F., McLean, I. S., & Najarro, F. 1997, *ApJ*, 486, 420
 Galavis, M. E., Mendoza, C., & Zeippen, C. J. 1995, *A&AS*, 111, 347
 Greenhouse, M. A., Feldman, U., Smith, H. A., Klapisch, M., Bhatia, A. K., & Bar-Shalom, A. 1993, *ApJS*, 88, 23
 Greenhouse, M. A., Grasdalén, G. L., Woodward, C. E., Benson, J., Gehrzt, R. D., Rosenthal, E., & Skrutskie, M. F. 1990, *ApJ*, 352, 307
 Grasdalén, G. L., & Joyce, R. R. 1976, *Nature*, 259, 187
 Hoffleit, D., & Jaschek, C. 1982, *The Bright Star Catalogue* (New Haven: Yale Univ. Obs.)
 Iijima, T., Rosino, L., & Della Valle, M. 1998, *A&A*, 338, 1006
 Koornneef, J. 1983, *A&A*, 128, 84
 Kurucz, R. L. 1991, in *Precision Astronomy and Astrophysics of the Galaxy*, ed. A. G. Davis Philip, A. R. Upgren, & K. A. Janes (Schenectady: Davis), 1
 Lutz, D., Krabbe, A., & Genzel, R. 1993, *ApJ*, 418, 244
 Lynch, D. K., Rossano, G. S., Rudy, R. J., & Puetter, R. C. 1995, *AJ*, 110, 2274
 Lynch, D. K., Rudy, R. J., Venturini, C. C., Mazuk, S., & Puetter, R. C. 2001, *AJ*, 122, 2013
 Mason, C. G., Gherz, R. D., Woodward, C. E., Smilowitz, J. B., Greenhouse, M. A., Hayward, T. L., & Houck, J. R. 1996, *ApJ*, 470, 577
 Nahar, S. N., Delahaye, F., Pradhan, A. K., & Zeippen, C. J. 2000, *A&AS*, 144, 141
 Nahar, S. N., & Pradhan, A. K. 1996, *A&AS*, 119, 509
 Osterbrock, D. E. 1989, *Astrophysics of Gaseous Nebulae and Active Galactic Nuclei* (Mill Valley: University Science Books)
 Osterbrock, D. E., Tran, H. D., & Villeux, S. 1992, *ApJ*, 389, 305
 Rossano, G. S., Rudy, R. J., Puetter, R. C., & Lynch, D. K. 1994, *AJ*, 107, 1128
 Rudy, R. J., Lynch, D. K., Mazuk, S., Puetter, R. C., & Dearborn, D. S. 2001, *AJ*, 121, 362
 Rudy, R. J., Puetter, R. C., & Mazuk, S. 1999, *AJ*, 118, 666
 Storey, P. J., & Hummer, D. G. 1995, *MNRAS*, 272, 41
 Wagner, R. M., & DePoy, D. L. 1996, *ApJ*, 467, 860 (WD96)
 Woodward, C. E., et al. 1995, *ApJ*, 438, 921
 Zhang, H. L. 1996, *A&AS*, 119, 523
 Zhang, H. L., & Pradhan, A. K. 1997, *A&AS*, 126, 373